

Hadron Structure on the Lattice

Harvey B. Meyer^{1,a}

Institut für Kernphysik, Johannes Gutenberg Universität Mainz, 55099 Mainz, Germany

Abstract. A few chosen nucleon properties are described from a lattice QCD perspective: the nucleon sigma term and the scalar strangeness in the nucleon; the vector form factors in the nucleon, including the vector strangeness contribution, as well as parity breaking effects like the anapole and electric dipole moment; and finally the axial and tensor charges of the nucleon. The status of the lattice calculations is presented and their potential impact on phenomenology is discussed.

1 Introduction

One of the goals of lattice QCD simulations is to calculate the properties of hadrons from first principles and to understand how their structure arises from QCD. In this review we will focus on the structure of the nucleon, because it is the only stable hadron in the Standard Model and because a precise knowledge of its structure has implications for new physics searches.

Many properties of the nucleon can be calculated on the lattice, see [1] for a comprehensive review. In addition one has the option not available experimentally to vary the quark masses, which can help to make contact with idealized models. This ability represents one more handle to explore ‘the internal landscape of the nucleon’, to use the expression of the 2007 NSAC¹ Long Range Plan.

It is useful to distinguish between those properties that are well determined experimentally, and others where the lattice can potentially be as accurate or more accurate than phenomenology in the foreseeable future. The first class then serves as a set of control quantities; these are for instance the electromagnetic form factors and the axial charge of the proton. The second class contains for instance the sigma term, the vector strangeness form factor and the isovector tensor charge, which are much harder to extract accurately from experiments. However, in order to increase confidence in the lattice predictions for the second class of observables, it is necessary to make contact between the lattice predictions of the ‘control quantities’ and their experimental values.

It should be noted that calculations in the mesonic sector are at a more advanced stage, in the sense that several benchmark quantities match the phenomenological determinations, and have in some cases even overtaken them in accuracy. Examples thereof are f_K/f_π , form factors of pseudoscalar mesons, and low-energy constants of chiral perturbation theory [2,3].

^a e-mail: meyerh@kph.uni-mainz.de

¹ The U.S. Nuclear Science Advisory Committee.

Rather than attempting to give a comprehensive overview of lattice nucleon structure calculations, we discuss three topics: the nucleon mass decomposition and the associated scalar matrix elements; the standard electromagnetic form factors as well as the anapole and electric dipole moments; and finally the axial and tensor charges. In this way both mature calculations and exploratory studies will be covered.

2 The nucleon mass decomposition

Let $T_{\mu\mu}$ be the trace of the energy-momentum tensor,

$$T_{\mu\mu} = \frac{\beta(g)}{2g} G_{\mu\nu}^a G_{\mu\nu}^a + (m_u \bar{u}u + m_d \bar{d}d) + m_s \bar{s}s + \dots \quad (1)$$

with $\beta(g) = -b_0 g^3 + \dots$ and $b_0 = (\frac{11}{3}N_c - \frac{2}{3}N_f)(4\pi)^{-2}$. The expectation value of this operator on a nucleon at rest yields the nucleon mass [4,5],

$$\frac{\langle N | \int d^3x T_{\mu\mu} | N \rangle}{\langle N | N \rangle} = M_N. \quad (2)$$

Each contributing operator in (1) is gauge invariant and renormalization group invariant. It is of interest to calculate the relative size of these contributions to Eq. (2). Recently, there have been several lattice calculations of the nucleon sigma term, defined as

$$\sigma_N \equiv m_{ud} \langle \bar{u}u + \bar{d}d \rangle, \quad m_{ud} \equiv \frac{1}{2}(m_u + m_d). \quad (3)$$

The expectation value refers to the operator evaluated on the zero-momentum nucleon state, with the vacuum expectation value subtracted. In a mass-independent scheme, the quantity can also be obtained from the Feynman-Hellmann theorem,

$$\sigma_N = m_q \frac{\partial}{\partial m_q} M_N. \quad (4)$$

To leading order in chiral perturbation theory, the derivative with respect to the quark mass can be replaced by the derivative with respect to the pion mass,

$$\sigma_N \simeq \frac{1}{2} M_\pi \frac{\partial}{\partial M_\pi} M_N \equiv \tilde{\sigma}_N. \quad (5)$$

2.1 The nucleon sigma term and the quark mass dependence of the nucleon mass

In phenomenology, the light-quark scalar form factor can be related to the πN scattering amplitude at the Cheng-Dashen point $t = +2m_\pi^2$ [6]. Correcting to get the scalar matrix element at zero momentum transfer, the value obtained is $\sigma_N = 45\text{MeV}$ [7]. More recent experimental data leads to larger values [8].

On the lattice, the nucleon mass has been calculated for a range of pion masses. This set of data points is fitted with a functional form provided by a chiral effective theory. Via Eq. (5) the parameter $\tilde{\sigma}_N$ is one of the fit parameters. In this way, the LHP collaboration extracted the value $\tilde{\sigma}_N \simeq 42(17)\text{MeV}$ in an NNLO SU(2) covariant baryon ChPT formula without explicit delta-baryon degrees of freedom [9] (see top left panel of Fig. 1). The lightest pion mass reached is 295MeV . When the $N - \Delta$ mass splitting is treated as being small and the delta as being an active degree of freedom, Walker-Loud et al. find $\tilde{\sigma}_N \simeq 84(27)\text{MeV}$ [9]. The latter fit is however

poorly constrained, due to the many parameters involved in the fit; for instance, the nucleon-delta coupling was set to $c_A = 1.5(3)$.

Young and Thomas [10] find $\tilde{\sigma}_N \simeq 47(10)\text{MeV}$ by fitting LHP [9] and PACS-CS [11] octet baryon spectrum data using a finite range regularization ansatz [12]. The ETM collaboration obtains $67(8)\text{MeV}$ in a two-flavor calculation with pion masses down to about 300MeV [13]. The JLQCD collaboration finds $\tilde{\sigma}_N = 52(2)(^{+20}_{-7})(^{+5}_{-0})\text{MeV}$ [14] in $N_f = 2$ QCD, where the first uncertainty is statistical, the second comes from the chiral extrapolation and the third is an estimate of finite-volume effects. The central value comes from fitting the pion mass dependence of the nucleon mass by a fourth-order polynomial in m_π , where the $O(m_\pi)$ vanishes and the coefficient of the m_π^3 term is known in terms of the axial charge g_A and the pion decay constant f_π . The BMW collaboration recently presented the result $\tilde{\sigma}_N \simeq 55(10)_{\text{stat}}\text{MeV}$ [15] using an ansatz based on a modified integration contour in covariant baryon ChPT that exploits the approximate SU(3) flavor symmetry. The bottom right panel of Fig. (1) displays such a fit to the octet of baryons with 7 parameters and 40 data points. Different fit ansätze and ranges are estimated to lead to a systematic uncertainty of about 10MeV [15].

There is thus a satisfactory agreement among lattice calculations, as well as between $\tilde{\sigma}_N$ calculated on the lattice and σ_N obtained from experimental pion-nucleon scattering. The uncertainty on the lattice results to date are comparable to the phenomenological uncertainty and the two kinds of determinations are in good agreement. Of course it is desirable to improve the accuracy of these determinations, not least in view of the importance of this matrix element in dark matter searches [16].

2.2 Strangeness in the nucleon

The size of the strangeness term in Eq. (1) is often parametrized by

$$y \equiv \frac{2\langle \bar{s}s \rangle}{\langle \bar{u}u + \bar{d}d \rangle}, \quad (6)$$

where the expectation value has the same meaning as in Eq. (3).

In phenomenology, a standard way to estimate y is to extract the matrix element $\sigma_8 \equiv m_{\text{ud}}\langle \bar{u}u + \bar{d}d - 2\bar{s}s \rangle$ from the octet baryon spectrum. A benchmark ChPT estimate is $\sigma_8 \simeq 36(7)\text{MeV}$ [19,20]. The difference between σ_N and σ_8 is then attributed to the strange quarks, $\sigma_8 = \sigma_N(1-y)$. Gasser et al. thus estimated $y = 0.2$ in 1991 [7]. The more recent estimates from the πN scattering data [8] lead to a large value for y , 0.3–0.6. Such a large value is surprising from the quark model point of view.

In view of the large value and the large uncertainty on the phenomenological estimates of y , it is of interest to study this quantity ab initio using lattice computational techniques. Young and Thomas [10] found $\frac{\sigma_s}{M_N} = 0.033(16)(4)(2)$ at the same time as σ_N by fitting the baryon octet spectrum (as discussed in section 2.1). The calculations we review below have been done by evaluating directly the forward matrix element of $\bar{s}s$. We start with the recent results of the JLQCD collaboration [21]. It employs overlap fermions, which preserve a lattice form of chiral symmetry exactly [22]. On $N_f = 2$ ensembles (i.e. with a quenched strange quark), the JLQCD collaboration finds

$$\frac{\sigma_s}{M_N} \equiv \frac{m_s}{M_N} \langle N | \bar{s}s | N \rangle = 0.032(8)_{\text{stat}}(22)_{\text{syst}}. \quad (7)$$

Takeda of the JLQCD collaboration has also presented preliminary results for the same quantity calculated on $N_f = 2 + 1$ ensembles of overlap fermions [23],

$$\frac{\sigma_s}{M_N} = 0.013(12)(16). \quad (8)$$

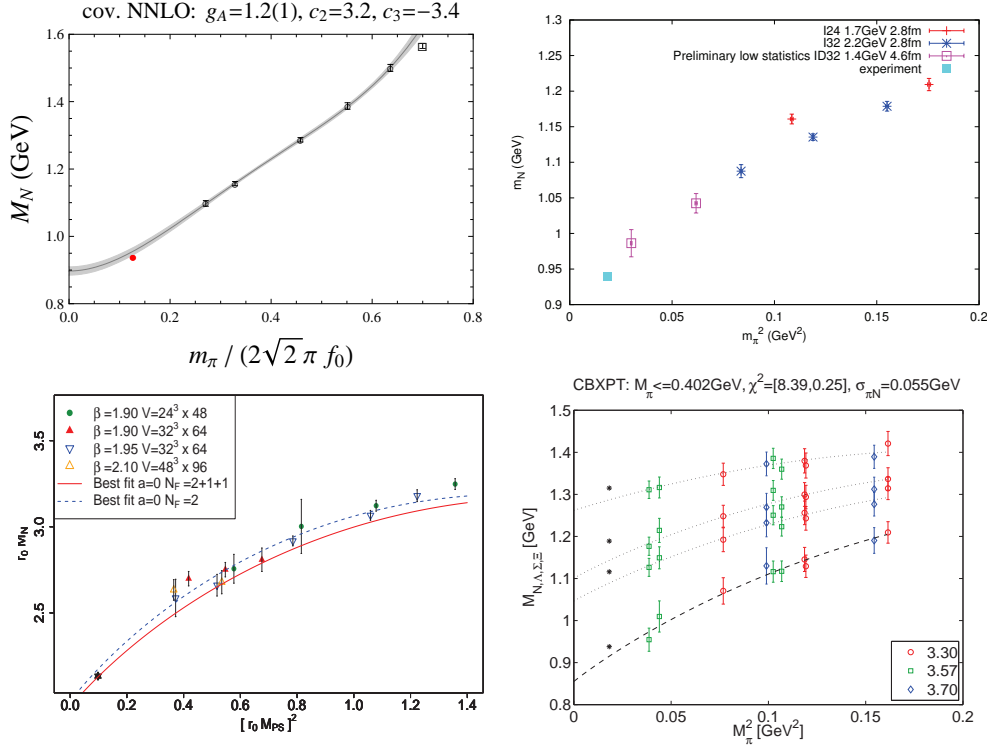


Fig. 1. Recent lattice calculations by four different collaborations of the pion mass dependence of the nucleon mass. **Top:** LHP ([9], $N_f = 2 + 1$, mixed action domain-wall/staggered) and RBC-UKQCD collaboration ([17], $N_f = 2 + 1$ domain-wall fermions). **Bottom:** ETM ([18], $N_f = 2 + 1 + 1$ twisted mass Wilson fermions) and BMW collaborations ([15], $2 + 1$ stout-smearred Wilson fermions).

Toussaint and Freedman [24] on the other hand find

$$\frac{\sigma_s}{M_N} = 0.063(6)(9) \quad (9)$$

using 2+1 flavors of Kogut-Susskind fermions.

Thus while there are still noticeable differences between the results, there is a consensus among these recent calculations that $\frac{\sigma_s}{M_N} < 0.08$, and possibly it is even much smaller. To put this into perspective, we note that in 2+1 flavor QCD, the result for a very massive strange quark would be $\sigma_s/M_N \simeq 2/29 \simeq 0.069$ [4,25]. At the physical value of the strange quark mass, the results reviewed above appears to be somewhat smaller. Finally we remark that the successive contributions of the charm, bottom and top quarks to the mass sum rule are not expected to decrease with the mass of the quarks, they are predicted in perturbation theory to be about 0.086, plus/minus 5% [25].

These results on the scalar strangeness can also be translated into predictions for the y parameter, if the quark mass ratio m_s/m_{ud} is known. Figure (2) is reproduced from [21], where this mass ratio was set to the value 27.4 for the conversion and the value for σ_N taken from [14]. The recent results lead us to the conclusion that $y < 0.1$, unlike some of the older calculations, which were affected by an uncontrolled operator mixing problem due to the lack of chiral symmetry on the lattice [26]. They also

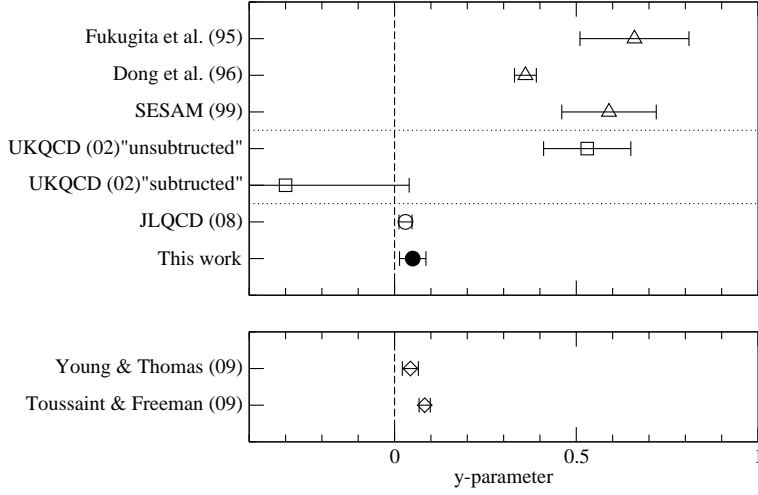


Fig. 2. Summary of lattice y parameter calculations from [21].

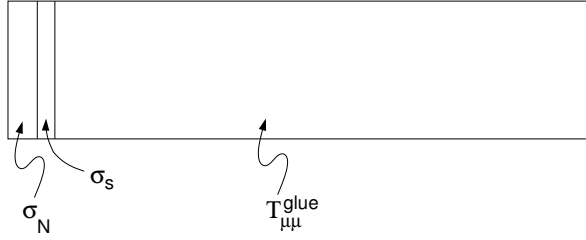


Fig. 3. Decomposition of the nucleon mass in $N_f = 2 + 1$ QCD based on Eq. (1) according to the lattice QCD results of the JLQCD collaboration [14,21].

suggest that the aforementioned phenomenological determinations of y overestimate this parameter.

2.3 Summary

The relative size of the light-quark, strange-quark and glue contributions to the nucleon mass is illustrated in Fig. (3). The central values used in this figure are those of the JLQCD collaboration [14,21]. The relative uncertainty on σ_N and σ_s is still large. It is interesting that the light quarks and the strange quark make contributions of the same order, both of them being small compared to the gluonic contribution. This weak dependence on the quark mass is the qualitative behavior expected in the heavy-quark regime, and appears to extend down into the light-quark regime.

It is worth noting that in the 1990's, the quark mass contribution to the nucleon mass was estimated to be quite large. For instance, Ji put forward the numbers [5]

$$\frac{1}{M_N}(\sigma_N + \sigma_s) \simeq 0.11, \quad 0.17,$$

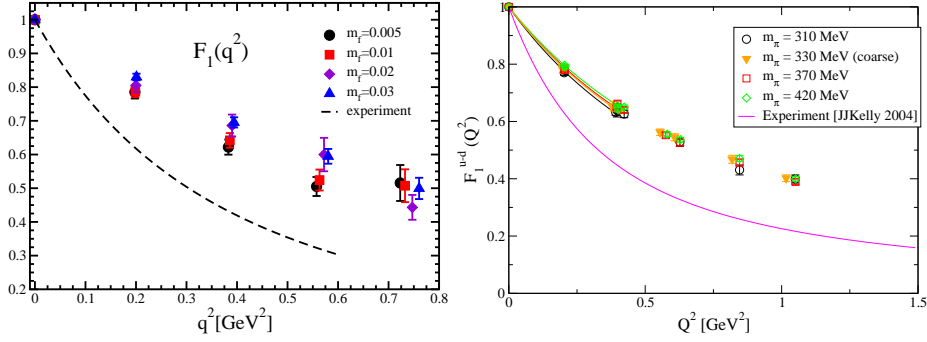


Fig. 4. The isovector Dirac form factor F_1^{u-d} . Left: $N_f = 2 + 1$ domain-wall-fermion calculation by the RBC-UKQCD collaboration at a lattice spacing $a = 0.114\text{fm}$ and for $m_\pi \geq 350\text{MeV}$ [27]. Right: calculation by Syritsyn et al. (LHP collaboration [28]) at a lattice spacing $a = 0.084\text{fm}$ and for $m_\pi \geq 310\text{MeV}$ on configurations generated by the RBC-UKQCD collaboration [29]. The lattice data is compared to Kelly's parametrization [30].

where the two values come from treating the strange quark mass as heavy and light, respectively. The JLQCD result, with the strange quark partially quenched [14,21], is smaller, $0.09(3)$.

3 Electromagnetic form factors and the anapole and dielectric moments

In this section we discuss the matrix elements of the vector current between two nucleon states. We start with the standard case where no parity violating effects are present (such as the θ angle or the weak force). First, we review the form factors of the isovector current, which is technically easier to calculate on the lattice. Then we present some recent results on the strangeness form factors. We then move on to discuss the anapole moment and the electric dipole moment of the nucleon, reviewing the few existing calculations and commenting on the prospects of future calculations.

The matrix elements of the vector current between two nucleon states (with no source of parity violation) reads

$$\langle p', s' | J^\mu | p, s \rangle = \bar{u}_{s'}(p') \Gamma^\mu(q^2) u_s(p), \quad (10)$$

$$\Gamma^\mu(q^2) = \gamma^\mu F_1(q^2) + i\sigma^{\mu\nu} \frac{q_\nu}{2M_N} F_2(q^2) \quad (11)$$

with $\sigma^{\mu\nu} = \frac{i}{2}[\gamma^\mu, \gamma^\nu]$. Furthermore we will show results for the Sachs form factors,

$$G_E(Q^2) = F_1(Q^2) - \frac{Q^2}{(2M_N)^2} F_2(Q^2), \quad (12)$$

$$G_M(Q^2) = F_1(Q^2) + F_2(Q^2). \quad (13)$$

3.1 Isovector contributions

Calculating the nucleon form factors of the vector isospin current J_μ^a is an important task for lattice QCD. The disconnected Wick contraction diagrams cancel for degenerate u, d quarks, which simplifies the calculation considerably. Ultimately the

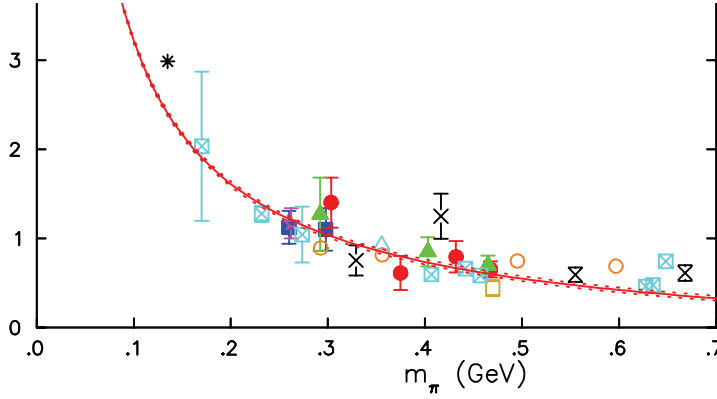


Fig. 5. The chiral extrapolation of the combination $(r_2)^2 \kappa_v$ in units of $(\text{fm}^2 \mu_N)$, Fig. from [32]. Data from $N_f = 2$ twisted mass fermions [33] ($a = 0.089\text{fm}$: filled red circles for $L = 2.1\text{fm}$ and filled blue squares for $L = 2.8\text{fm}$; $a = 0.070\text{fm}$: filled green triangles for $L = 2.2\text{fm}$; $a = 0.056\text{fm}$: purple star for $L = 2.7\text{fm}$ and open yellow square for $L = 1.8\text{fm}$); $N_f = 2+1$ domain-wall fermions with $a = 0.114\text{fm}$ and $L = 2.7\text{fm}$ [27] (crosses); mixed action calculation [34] (open orange circles for $L = 2.5\text{fm}$ and open cyan triangles for $L = 3.5\text{fm}$); and $N_f = 2$ $O(a)$ improved Wilson fermions [35] (cyan cross-in-square).

goal is to make contact with the experimental measurements, and unless this contact is made, the degree of confidence one will have in lattice calculations of nucleon structure will be limited. A number of collaborations have carried out calculations of the isovector form factors for pion masses down to about 280MeV . A few calculations exist at lighter pion masses, but they remain exploratory, either because of the lack of control of finite-volume effects, or because the statistical fluctuations on the nucleon correlator increases drastically.

As an example, Fig. (4) displays the isovector Dirac form factor calculated with $2+1$ flavors of domain-wall fermions [27,28]. Our main observations are the following. A high level of statistical accuracy has been achieved in the displayed range of pion masses. Secondly the pion mass dependence of the form factor is very weak between 500 and 300MeV , and in this range the form factor falls off much more slowly in Q^2 than the experimentally measured form factor. Thirdly, the dipole form $1/(1 + Q^2/M_D^2)^2$ provides a good fit up to $Q^2 \approx 1\text{GeV}^2$. The pion mass dependence of the dipole mass M_D is of physical interest. It is natural to normalize it by the corresponding nucleon mass, however this does not resolve the difficulty of extrapolating the lattice data points [31]. The dipole mass can also be normalized by the ρ meson mass computed at the same quark mass. This ratio turns out to be significantly larger than it is in the real world [31], about 1.5 instead of 1.1 .

The small Q^2 region of the form factors is parametrized in leading order by the anomalous magnetic moment as well as the Dirac and Pauli radii, for instance $-6 \frac{dF_1}{dQ^2} |_{Q^2=0} = (r_1)^2 = \frac{12}{M_D^2}$. At present these have to be extrapolated to the physical pion mass. At sufficiently small pion masses, the functional form is predicted by chiral effective theory. The asymptotic chiral behavior of the Dirac and Pauli radii as well

as of the anomalous magnetic moment are

$$(r_1^v)^2 \sim \log m_\pi, \quad (14)$$

$$(r_2^v)^2 \sim m_\pi^{-1}, \quad (15)$$

$$\kappa_v \equiv F_2(0) \sim \text{cst}. \quad (16)$$

More precisely, as an example of the expressions involved, we give here [36]

$$\kappa_v(m_\pi)(r_2^v)^2 = \frac{g_A^2 M_N}{8\pi f_\pi^2 m_\pi} + \frac{c_A^2 M_N}{9\pi^2 f_\pi^2 \sqrt{\Delta^2 - m_\pi^2}} \log \left[\frac{\Delta}{m_\pi} + \sqrt{\frac{\Delta^2}{m_\pi^2} - 1} \right], \quad (17)$$

where $f_\pi \simeq 86\text{MeV}$ in the chiral limit, $\Delta \simeq 293\text{MeV}$ is the nucleon-delta mass splitting and c_A is the axial nucleon-delta coupling. In this ‘small-scale expansion’ power counting scheme, the delta resonance is an ‘active’ degree of freedom. The combination (17) has the advantage that one low-energy constant drops out. The extrapolation of this expression is illustrated in Fig. (5) [32]. The data of several collaborations appear on the figure. The coefficient of the $1/m_\pi$ term is expressed in terms of well-known quantities, and the lattice data and the experimental data point cannot be joined by the ansatz (17). The validity of the fit ansatz is presumably limited to pion masses much smaller than those at which accurate lattice data is currently available. An ansatz to tame the strong pion mass dependence has been proposed [37], where the form at higher quark masses is inspired by quark models. However lattice data at smaller pion masses will clearly be required for a controlled calculation of the proton radii and anomalous magnetic moment.

3.2 Strangeness vector form factor: Wick-disconnected contributions

The number of calculations of the strange quark contribution to the electromagnetic form factor is much more limited. At a numerical level they are important as a technical step towards calculating the Wick-disconnected diagram contributions to the u, d form factors. At a physics level they teach us about the spatial distribution of strange quark-antiquark pairs in the nucleon.

The Wick contraction of the three-point function that yields the strange form factor is purely disconnected. This means that the expectation value of the strange vector current on nucleon states is mediated entirely by gluons. As a consequence, the Monte-Carlo variance associated with the operator diverges as $1/a^6$, where a is the lattice spacing. This is the main reason Wick-disconnected diagrams are difficult to calculate. An additional difficulty is that in order to select two of the initial- and final-state momenta P, P' and $Q = P' - P$ exactly on the lattice, the strange quark propagator in the background gauge field would have to be computed for every point in space, which is prohibitively expensive. This difficulty is circumvented by obtaining the propagators stochastically. This is advantageous because the noise associated with this procedure can be reduced below the noise level associated with the fluctuations of the gauge fields at a cost which is still moderate compared to the cost of generating the gauge fields.

The calculation of the χQCD collaboration is displayed in Fig. (6, Ref. [38]). It is restricted to the regime of heavy pion masses $m_\pi \geq 600\text{MeV}$, but even allowing for a conservative error band for the chiral extrapolation, the results suggest that both the electric and magnetic form factors are very small. This is qualitatively confirmed by a very recent calculation by Babich et al. (Fig. 7, Ref. [39]) at the lower pion mass of 416MeV . There is some indication in both calculations that G_M^s is negative.

Altogether these lattice results indicate that the strangeness form factors of the nucleon are very small, even smaller than the bounds obtained by recent experiments.

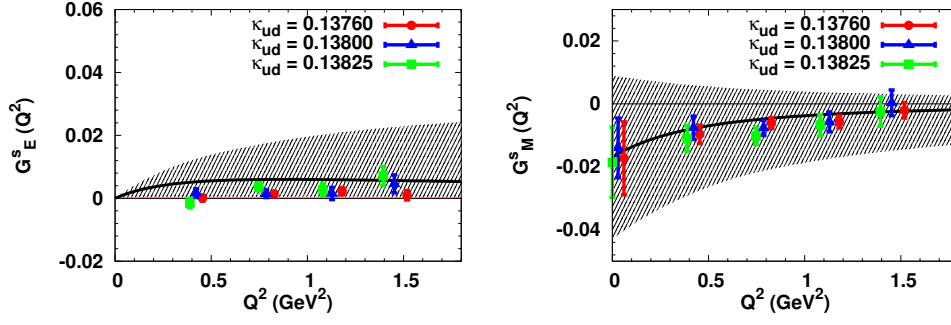


Fig. 6. Strangeness Sachs form factors calculated at $m_\pi \geq 600\text{MeV}$ and at a lattice spacing $a = 0.12\text{fm}$ in $N_f = 2 + 1$ QCD [38].

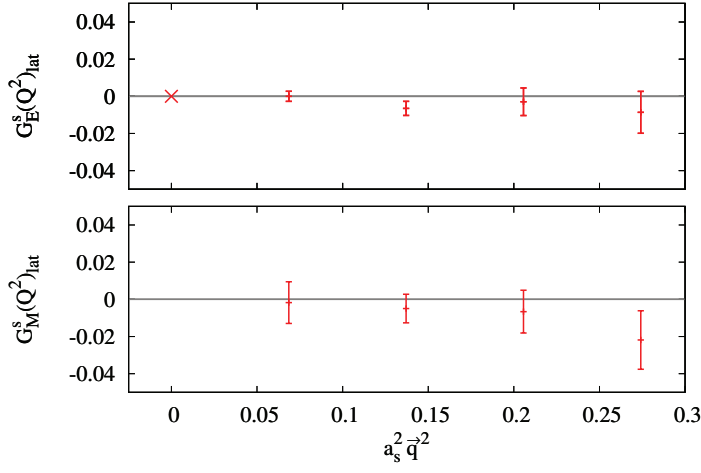


Fig. 7. Strangeness Sachs form factors calculated on an anisotropic lattice with a spatial lattice spacing of $a_s = 0.108(7)\text{fm}$ and at $m_\pi = 416(36)\text{MeV}$ [39].

For comparison, the PVA4 experiment at MAMI quotes $G_M^s(0.22\text{GeV}^2) = -0.14 \pm 0.11 \pm 0.11$ [40]. It will have to be seen whether the strangeness form factors remain as small when the pion mass approaches its physical value.

3.3 Anapole form factor

There are several contexts in which parity violating effects in nucleon structure measurements are important. One example is the measurement of a neutron electric dipole moment [41]. Another is the parity violating scattering experiments which aim at measuring the weak charge of the proton or its strangeness form factor [42].

If parity is not a good quantum number, two additional form factors are necessary to parametrize the matrix elements of the vector current on a spin 1/2 bound state,

$$\begin{aligned} \Gamma^\mu(q^2) = & \gamma^\mu F_1(q^2) + i\sigma^{\mu\nu} \frac{q_\nu}{2M_N} F_2(q^2) + (\gamma^\mu \gamma_5 q^2 - 2M_N \gamma_5 q^\mu) F_A(q^2) \\ & + \sigma_{\mu\nu} \gamma_5 \frac{q_\nu}{2M_N} F_3(q^2). \end{aligned} \quad (18)$$

The quantity $F_A(0)$ measures the anapole moment of the nucleon. It describes the fact that a matrix element of the vector current can yield a result which has an axial-vector tensor structure. Sources of a non-zero F_A form factor are the weak force or a potential θ term in QCD. Although we are not aware of any lattice calculations of F_A , the contribution induced by a small θ term can be computed along the same lines as the electric dipole form factor F_3 calculation described in the next section.

3.4 Electric dipole moment

The electric dipole moment is determined by the form factor F_3 at vanishing momentum transfer,

$$d_N = \frac{F_3(0)}{2M_N}. \quad (19)$$

When the only source of parity violation is the θ -term of QCD, the electric dipole moment has an expansion

$$d_N = d_N^{(1)}\theta + \mathcal{O}(\theta^3), \quad (20)$$

and the goal of lattice simulations is to calculate $d_N^{(1)}$. Together with experimental bounds on d_N , this quantity allows one to derive an upper bound on θ . Currently, the experimental bound is $|d_N| < 2.9 \cdot 10^{-26} e \cdot \text{cm}$ [43], and experiments are being planned to reach an accuracy of (a few) $\cdot 10^{-28} e \cdot \text{cm}$ (see [41] for a review of these experiments). The Standard Model contribution to the neutron EDM is less than $10^{-31} e \cdot \text{cm}$ [44].

One method to obtain $d_N^{(1)}$ is to calculate the form factor F_3 , and extrapolate it to $Q^2 = 0$. As far as the Wick-connected diagrams are concerned, smaller momentum transfers can be reached by using twisted boundary conditions [45]. There is an alternative method. In a constant and uniform electric field \mathbf{E} , a shift in energy of the nucleon state with spin \mathbf{S} takes place,

$$\Delta E = d_N \mathbf{S} \cdot \mathbf{E} + \dots \quad (21)$$

The dots refer to terms quadratic in the electric field (sensitive to polarizabilities) and higher.

There are several methods to simulate QCD at small θ . One is to explicitly Taylor-expand the observable around $\theta = 0$,

$$\begin{aligned} \langle \mathcal{O} \rangle_\theta &= \frac{1}{Z(\theta)} \int \mathcal{D}A_\mu \mathcal{D}\bar{\psi} \mathcal{D}\psi \mathcal{O} e^{-S[A, \psi, \bar{\psi}] - i\theta \int d^4x \frac{g^2}{32\pi^2} \text{Tr}[G(x)\tilde{G}(x)]} \\ &\simeq \langle \mathcal{O} \rangle_0 - i\theta \langle Q\mathcal{O} \rangle_0. \end{aligned} \quad (22)$$

In QCD at $\theta = 0$, the topological charge fluctuates around zero with a second moment

$$\frac{\langle Q^2 \rangle}{V} = \frac{f^2 m_\pi^2}{8} + \dots \quad (23)$$

| | $F_3(q^2)$ | $\Delta E = d_N \mathbf{S} \cdot \mathbf{E}$ |
|-----------|---|---|
| Taylor | Shintani et al ($N_f = 2+1$) [47]; Blum et al [48] | Shintani et al ($N_f = 2+1$) [49]; Shintani et al [50] |
| $i\theta$ | Horsley et al [45] | |

Table 1. Different lattice methods to calculate $d_N^{(1)}$. The calculation of Horsley et al. used twisted boundary conditions on the fermion fields. When not indicated, the flavor content is $N_f = 2$.

where we have indicated the leading chiral behavior of $\langle Q^2 \rangle$ with $f \approx 130\text{MeV}$ [46] and V denotes the four-volume.

The other method involves simulating QCD at imaginary θ , where no sign problem occurs. More precisely, the angle θ is rotated into a mass term,

$$S_F = \bar{\psi} \{D + \bar{m} + i(\bar{\theta}/N_f)\gamma_5 \bar{m}\} \psi, \quad \bar{m} = \cos(\bar{\theta}/N_f), \quad \bar{\theta} = N_f \tan(\theta/N_f).$$

Then one sets $\bar{\theta} \doteq -i\bar{\theta}^I$, θ^I real. The situation is similar to the case of a baryon chemical potential.

A further important aspect of the calculation is to take into account the change in the polarization tensor of a nucleon propagator when the theta angle is switched on (see the discussion in [47,48]).

The available results in the $N_f = 2$ theory, which should be regarded as preliminary, are summarized as follows,

- Blum et al. 2005 [48]: $d_N^{(1)} \lesssim 20 \cdot 10^{-3} e \text{ fm}$;
- QCDSF 2008 [45]: $d_N^{(1)} \lesssim 50 \cdot 10^{-3} e \text{ fm}$.

The results were obtained at a quark mass only slightly smaller than the physical strange quark mass. The results obtained directly on the lattice thus provide a relatively loose bound compared to the magnitude of the pion loop contribution to $d_N^{(1)}$ (Crewther et al. [51]),

$$d_N^{(1)} \approx 3.6 \cdot 10^{-3} e \cdot \text{fm}. \quad (24)$$

In the future, when an actual value for $d_N^{(1)}$ is obtained, the chiral extrapolation of $d_N^{(1)}$ will however be strongly constrained by the fact that it vanishes in the chiral limit [51],

$$d_N^{(1)} \sim m_\pi^2 \log m_\pi^2. \quad (25)$$

Therefore calculating $d_N^{(1)}$ on the lattice remains a challenging but realistic and important goal.

4 Axial and tensor charge of the nucleon

The isovector axial charge is the forward matrix element of the axial current on a polarized nucleon,

$$\langle P, S | A_\mu^a | P, S \rangle = \bar{U}(P, S) \gamma_\mu \gamma_5 \frac{\tau^a}{2} U(P, S) \cdot g_A. \quad (26)$$

It is related to helicity parton distribution functions by the Bjorken sum rule

$$g_A = \int_0^1 dx (\Delta q(x) + \Delta \bar{q}(x)). \quad (27)$$

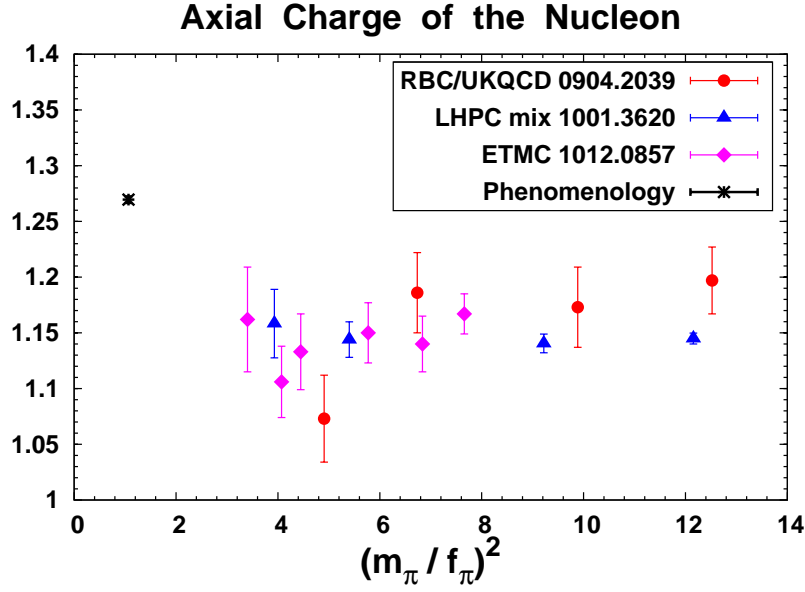


Fig. 8. Summary of several recent lattice g_A calculations.

We focus here on the isovector combination, which is measured in neutron β decay with the result $g_A^{\text{expt}} = 1.2695(29)$ in units of the vector coupling g_V . The isovector axial charge $g_A \equiv g_A^3$ does not have a renormalization scale dependence, although the higher moments of $\Delta q(x)$ do.

In several respects, g_A is a cornerstone of nucleon physics. The Adler-Weisberger sum rule relates the departure of g_A from unity to an integral over the difference between the π^+p and π^-p scattering cross sections, where the delta features as a prominent resonance. Furthermore in the chiral limit the axial charge is directly related to the pion-nucleon coupling strength by the Goldberger-Treiman relation $g_A = f_\pi g_{\pi NN} / M_N$.

A summary of recent published lattice calculations is given in Fig. (8). The results are very weakly pion-mass dependent, and lie at a level of 1.15, i.e. about 10% below the phenomenological value. The displayed statistical errors are significantly smaller than that, and it therefore remains to be seen whether and how contact is made with the phenomenological value. A discussion of the sources of systematic error is given by H. Wittig in these same proceedings.

The chiral expansion of g_A has been carried out to higher order. The delta resonance is thought to influence the pion mass dependence of g_A , since the gap between the nucleon and the delta is about equal to the pion mass when $m_\pi = 350\text{MeV}$ [9].

In the small-scale expansion counting scheme, the expression takes the form [52]

$$g_A(m_\pi) = g_A - \frac{g_A^3 m_\pi^2}{16\pi^2 f_\pi^2} + 4m_\pi^2 \left\{ C(\lambda) + \frac{c_A^2}{4\pi^2 f_\pi^2} \left[\frac{155}{972} g_1 - \frac{17}{36} g_A \right] + \gamma \log \frac{m_\pi}{\lambda} \right\} \\ + \frac{4c_A^2 g_A}{27\pi f_\pi^2 \Delta} m_\pi^3 + \frac{8c_A^2 g_A m_\pi^2}{27\pi^2 f_\pi^2} \left[1 - \frac{m_\pi^2}{\Delta^2} \right]^{\frac{1}{2}} \log R \quad (28)$$

$$+ \frac{c_A^2 \Delta^2}{81\pi^2 f_\pi^2} (25g_1 - 57g_A) \left\{ \log \frac{2\Delta}{m_\pi} - \left[1 - \frac{m_\pi^2}{\Delta^2} \right]^{\frac{1}{2}} \log R \right\},$$

$$\gamma = \frac{1}{16\pi^2 f_\pi^2} \left[\frac{50}{81} c_A^2 g_1 - \frac{1}{2} g_A - \frac{2}{9} c_A^2 g_A - g_A^3 \right], \quad (29)$$

$$R = \frac{\Delta}{m_\pi} + \left[\frac{\Delta^2}{m_\pi^2} - 1 \right]^{\frac{1}{2}}. \quad (30)$$

The couplings g_1 and c_A are respectively the axial delta-delta and the axial nucleon-delta coupling, while Δ is the nucleon-delta mass splitting in the chiral limit. In addition, when the Δ baryon is below the $N\pi$ threshold, as is the case in most lattice calculations to date, $\sqrt{\Delta^2 - m_\pi^2} \log R(m_\pi)$ is substituted by $-\sqrt{m_\pi^2 - \Delta^2} \arccos(\Delta/m_\pi)$. As usual, it is not a priori known what the effective radius of convergence is. We remark that the $m_\pi^2 \log m_\pi$ term has a negative coefficient (most easily seen by setting $c_A = g_1 = 0$), which means that the axial coupling in the chiral limit is reached from above. This implies that the axial coupling must have a local maximum as a function of m_π^2 if we imagine a curve going through the lattice data points and the phenomenological value. Such a structure remains to be seen explicitly in the lattice data.

The other flavor-octet linear combination of axial charges, g_A^8 (proportional to the linear combination $(u + d - 2s)$, where the SU(3) generators are normalized according to $\text{Tr} \{ \lambda^a \lambda^b \} = 2\delta^{ab}$) is of course also of interest, particularly in the context of the quark spin contributions to the nucleon spin [53]. On the lattice, in addition to Wick-connected diagrams, it requires calculating the difference of the light-quark and strange-quark disconnected diagrams. The latter however cancel at an $SU(3)_f$ symmetric point. The connected diagrams at such a point were calculated for instance by the LHP collaboration with all three quark masses equal to the physical strange quark mass. In that case the result is $g_A^8/g_A^3 = 0.315(9)$ [54]. The value in this fairly massive theory is surprisingly close to the value extracted from phenomenological octet baryon axial charges [55].

4.1 The tensor charge

Transversity is an active topic of research in deep inelastic scattering and related experiments, see [61] for a review. Similar to the axial charge for the longitudinal polarization, the tensor charge is the forward value of the antisymmetric-tensor form factor

$$\langle P, S | \bar{q} i\sigma_{\alpha\beta} q | P, S \rangle = \bar{U}(P, S) i\sigma_{\alpha\beta} U(P, S) \cdot g_T. \quad (31)$$

In terms of the transversity parton distribution functions, it corresponds to

$$g_T = \int_0^1 dx (\delta q(x) - \delta \bar{q}(x)), \quad (32)$$

i.e. it measures the x -average of the transverse polarization of quarks (minus that of the antiquarks) in a transversely polarized, fast moving proton. The fact that quarks

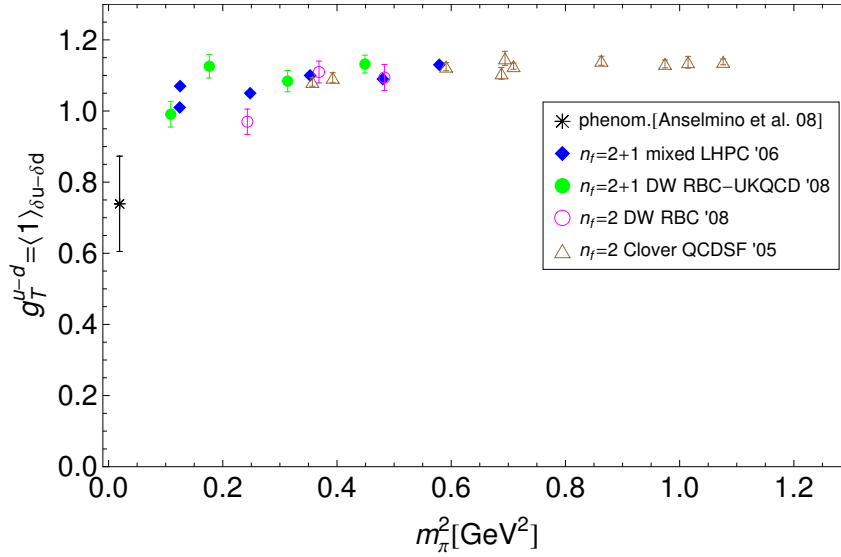


Fig. 9. Summary of several recent lattice g_T calculations [1]. The phenomenological estimate is from [56]. The references for the lattice calculations are in the same order as the caption [57], [58], [59], [60].

and antiquarks appear with opposite signs is physically significant. Here too we focus on the isovector combination. Unlike the axial charge, the tensor charge has a renormalization scale dependence. Figure (9) displays lattice results renormalized at an $\overline{\text{MS}}$ scale of 2GeV. Here the situation is opposite to the axial charge, in that the lattice data points at $m_\pi \gtrsim 280\text{MeV}$ are more accurate than the phenomenological value of the tensor charge. It is intriguing that the lattice data points for g_A and g_T are very close in value at a given pion mass (an observation already made in [62]), since in a non-relativistic theory they would be equal. The phenomenological values of g_A and g_T on the other hand are clearly split on either side of unity.

5 Conclusion

Lattice calculations of nucleon structure are a vibrant area of research which complements the worldwide experimental efforts dedicated to unravel the structure of the nucleon. For some quantities, I expect that in the coming decade a higher precision will be achieved on the lattice than in experiments, for instance for the isovector tensor charge (see Fig. 9) or the strangeness vector form factors (Figs. 6, 7). For hyperons, the same computational techniques can be applied without any major additional difficulties [63], while in an experiment hyperons require a very different treatment.

With the development and improvement of techniques to handle Wick-disconnected diagrams (see for instance [64,65]), as they appear for instance in strangeness matrix elements, the range of quantities that can be studied is expanding significantly. At the same time, the results for some of the more ‘prosaic’ quantities such as the axial charge g_A or the electromagnetic form factors F_1^{u-d} , F_2^{u-d} absolutely need to be improved to the point where contact is convincingly made with the well-established experimental measurements. Once that is achieved the interplay of hadron structure experiments and lattice calculations could be extremely fruitful.

I would like to thank Michael Ostrick for organizing a very stimulating Symposium on ‘Many-body structure of strongly interacting systems’ and more widely my colleagues at the Institute of Nuclear Physics in Mainz for a friendly work environment.

References

1. P. Hagler, *Hadron structure from lattice quantum chromodynamics*, *Phys. Rept.* **490** (2010) 49–175, [[arXiv:0912.5483](#)].
2. C. Sachrajda, *Phenomenology from the Lattice*, *PoS LATTICE2010* (2010) 018, [[arXiv:1103.5959](#)].
3. G. Colangelo, S. Durr, A. Juttner, L. Lellouch, H. Leutwyler, *et. al.*, *Review of lattice results concerning low energy particle physics*, [arXiv:1011.4408](#).
4. M. A. Shifman, A. Vainshtein, and V. I. Zakharov, *Remarks on Higgs Boson Interactions with Nucleons*, *Phys.Lett.* **B78** (1978) 443.
5. X.-D. Ji, *A QCD analysis of the mass structure of the nucleon*, *Phys.Rev.Lett.* **74** (1995) 1071–1074, [[hep-ph/9410274](#)].
6. T. P. Cheng and R. Dashen, *Is $su(2) \otimes su(2)$ a better symmetry than $su(3)$?*, *Phys. Rev. Lett.* **26** (Mar, 1971) 594–597.
7. J. Gasser, H. Leutwyler, and M. Sainio, *Sigma term update*, *Phys.Lett.* **B253** (1991) 252–259.
8. M. Pavan, I. Strakovsky, R. Workman, and R. Arndt, *The Pion nucleon Sigma term is definitely large: Results from a G.W.U. analysis of pi nucleon scattering data*, *PiN Newslett.* **16** (2002) 110–115, [[hep-ph/0111066](#)].
9. A. Walker-Loud, H.-W. Lin, D. Richards, R. Edwards, M. Engelhardt, *et. al.*, *Light hadron spectroscopy using domain wall valence quarks on an Asqtad sea*, *Phys.Rev.* **D79** (2009) 054502, [[arXiv:0806.4549](#)].
10. R. Young and A. Thomas, *Octet baryon masses and sigma terms from an $SU(3)$ chiral extrapolation*, *Phys.Rev.* **D81** (2010) 014503, [[arXiv:0901.3310](#)].
11. **PACS-CS Collaboration** Collaboration, S. Aoki *et. al.*, *2+1 Flavor Lattice QCD toward the Physical Point*, *Phys.Rev.* **D79** (2009) 034503, [[arXiv:0807.1661](#)].
12. R. D. Young, D. B. Leinweber, and A. W. Thomas, *Convergence of chiral effective field theory*, *Prog.Part.Nucl.Phys.* **50** (2003) 399–417, [[hep-lat/0212031](#)].
13. **European Twisted Mass Collaboration** Collaboration, C. Alexandrou *et. al.*, *Light baryon masses with dynamical twisted mass fermions*, *Phys.Rev.* **D78** (2008) 014509, [[arXiv:0803.3190](#)].
14. H. Ohki, H. Fukaya, S. Hashimoto, T. Kaneko, H. Matsufuru, *et. al.*, *Nucleon sigma term and strange quark content from lattice QCD with exact chiral symmetry*, *Phys.Rev.* **D78** (2008) 054502, [[arXiv:0806.4744](#)].
15. S. Durr, Z. Fodor, J. Frison, T. Hemmert, C. Hoelbling, *et. al.*, *Sigma term and strangeness content of the nucleon*, *PoS LATTICE2010* (2010) 102, [[arXiv:1012.1208](#)].
16. J. R. Ellis, K. A. Olive, and C. Savage, *Hadronic Uncertainties in the Elastic Scattering of Supersymmetric Dark Matter*, *Phys.Rev.* **D77** (2008) 065026, [[arXiv:0801.3656](#)].
17. **RBC Collaboration**, **UKQCD Collaboration** Collaboration, S. Ohta, *Nucleon structure from 2+1 flavor domain wall QCD at nearly physical pion mass*, [arXiv:1102.0551](#).
18. V. Drach, K. Jansen, J. Carbonell, M. Papinutto, and C. Alexandrou, *Low lying baryon spectrum with $N_f = 2 + 1 + 1$ dynamical twisted quarks*, *PoS LATTICE2010* (2010) 101, [[arXiv:1012.3861](#)].
19. J. Gasser and H. Leutwyler, *Quark Masses*, *Phys.Rept.* **87** (1982) 77–169.
20. B. Borasoy and U.-G. Meissner, *Chiral expansion of baryon masses and sigma terms*, *Annals Phys.* **254** (1997) 192–232, [[hep-ph/9607432](#)].
21. **JLQCD collaboration** Collaboration, K. Takeda *et. al.*, *Nucleon strange quark content from two-flavor lattice QCD with exact chiral symmetry*, [arXiv:1011.1964](#).

22. M. Luscher, *Exact chiral symmetry on the lattice and the Ginsparg-Wilson relation*, *Phys.Lett.* **B428** (1998) 342–345, [[hep-lat/9802011](#)].
23. **JLQCD Collaboration** Collaboration, K. Takeda *et. al.*, *Nucleon strange quark content in 2+1-flavor QCD*, *PoS LATTICE2010* (2010) 160, [[arXiv:1012.1907](#)].
24. **MILC Collaboration** Collaboration, D. Toussaint and W. Freeman, *The Strange quark condensate in the nucleon in 2+1 flavor QCD*, *Phys.Rev.Lett.* **103** (2009) 122002, [[arXiv:0905.2432](#)].
25. A. Kryjevski, *Heavy quark anti- q q matrix elements in the nucleon from perturbative QCD*, *Phys.Rev.* **D70** (2004) 094028, [[hep-ph/0312196](#)].
26. **UKQCD Collaboration** Collaboration, C. Michael, C. McNeile, and D. Hepburn, *The Strangeness content of the nucleon*, *Nucl.Phys.Proc.Suppl.* **106** (2002) 293–295, [[hep-lat/0109028](#)].
27. T. Yamazaki *et. al.*, *Nucleon form factors with 2+1 flavor dynamical domain-wall fermions*, *Phys. Rev.* **D79** (2009) 114505, [[arXiv:0904.2039](#)].
28. S. N. Syritsyn *et. al.*, *Nucleon Electromagnetic Form Factors from Lattice QCD using 2+1 Flavor Domain Wall Fermions on Fine Lattices and Chiral Perturbation Theory*, *Phys. Rev.* **D81** (2010) 034507, [[arXiv:0907.4194](#)].
29. **RBC-UKQCD Collaboration** Collaboration, C. Allton *et. al.*, *Physical Results from 2+1 Flavor Domain Wall QCD and SU(2) Chiral Perturbation Theory*, *Phys.Rev.* **D78** (2008) 114509, [[arXiv:0804.0473](#)].
30. J. J. Kelly, *Simple parametrization of nucleon form factors*, *Phys. Rev.* **C70** (2004) 068202.
31. H. B. Meyer, *Moments of GPDs and transverse-momentum dependent PDFs from the lattice*, *PoS DIS2010* (2010) 284, [[arXiv:1008.1181](#)].
32. C. Alexandrou, M. Brinet, J. Carbonell, M. Constantinou, P. Harraud, *et. al.*, *Nucleon electromagnetic form factors in twisted mass lattice QCD*, [arXiv:1102.2208](#).
33. **ETM Collaboration** Collaboration, C. Alexandrou *et. al.*, *Axial Nucleon form factors from lattice QCD*, *Phys.Rev.* **D83** (2011) 045010, [[arXiv:1012.0857](#)].
34. **LHPC Collaboration**, J. D. Bratt *et. al.*, *Nucleon structure from mixed action calculations using 2+1 flavors of asqtad sea and domain wall valence fermions*, [arXiv:1001.3620](#).
35. **QCDSF/UKQCD Collaboration** Collaboration, D. Pleiter *et. al.*, *Nucleon form factors and structure functions from $N(f)=2$ Clover fermions*, *PoS LATTICE2010* (2010) 153, [[arXiv:1101.2326](#)].
36. V. Bernard, H. W. Fearing, T. R. Hemmert, and U. G. Meissner, *The form-factors of the nucleon at small momentum transfer*, *Nucl.Phys.* **A635** (1998) 121–145, [[hep-ph/9801297](#)].
37. P. Wang, D. Leinweber, A. Thomas, and R. Young, *Chiral extrapolation of octet-baryon charge radii*, *Phys.Rev.* **D79** (2009) 094001, [[arXiv:0810.1021](#)].
38. T. Doi *et. al.*, *Nucleon strangeness form factors from $N_f=2+1$ clover fermion lattice QCD*, *Phys. Rev.* **D80** (2009) 094503, [[arXiv:0903.3232](#)].
39. R. Babich, R. C. Brower, M. A. Clark, G. T. Fleming, J. C. Osborn, *et. al.*, *Exploring strange nucleon form factors on the lattice*, [arXiv:1012.0562](#).
40. S. Baunack, K. Aulenbacher, D. Balaguer Rios, L. Capozza, J. Diefenbach, *et. al.*, *Measurement of Strange Quark Contributions to the Vector Form Factors of the Proton at $Q^2=0.22$ (GeV/c) 2* , *Phys.Rev.Lett.* **102** (2009) 151803, [[arXiv:0903.2733](#)].
41. J.-C. Peng, *Neutron Electric Dipole Moment Experiments*, *Mod.Phys.Lett.* **A23** (2008) 1397–1408, [[arXiv:0804.4254](#)].
42. D. Beck and R. McKeown, *Parity violating electron scattering and nucleon structure*, *Ann.Rev.Nucl.Part.Sci.* **51** (2001) 189–217, [[hep-ph/0102334](#)].
43. C. Baker, D. Doyle, P. Geltenbort, K. Green, M. van der Grinten, *et. al.*, *An Improved experimental limit on the electric dipole moment of the neutron*, *Phys.Rev.Lett.* **97** (2006) 131801, [[hep-ex/0602020](#)].
44. S. Dar, *The Neutron EDM in the SM: A Review*, [hep-ph/0008248](#).
45. S. Aoki, R. Horsley, T. Izubuchi, Y. Nakamura, D. Pleiter, *et. al.*, *The Electric dipole moment of the nucleon from simulations at imaginary vacuum angle θ* , [arXiv:0808.1428](#).

46. H. Leutwyler and A. V. Smilga, *Spectrum of Dirac operator and role of winding number in QCD*, *Phys.Rev.* **D46** (1992) 5607–5632.
47. E. Shintani, S. Aoki, N. Ishizuka, K. Kanaya, Y. Kikukawa, *et. al.*, *Neutron electric dipole moment from lattice QCD*, *Phys.Rev.* **D72** (2005) 014504, [[hep-lat/0505022](#)].
48. F. Berruto, T. Blum, K. Orginos, and A. Soni, *Calculation of the neutron electric dipole moment with two dynamical flavors of domain wall fermions*, *Phys.Rev.* **D73** (2006) 054509, [[hep-lat/0512004](#)].
49. E. Shintani, S. Aoki, N. Ishizuka, K. Kanaya, Y. Kikukawa, *et. al.*, *Neutron electric dipole moment with external electric field method in lattice QCD*, *Phys.Rev.* **D75** (2007) 034507, [[hep-lat/0611032](#)].
50. E. Shintani, S. Aoki, and Y. Kuramashi, *Full QCD calculation of neutron electric dipole moment with the external electric field method*, *Phys.Rev.* **D78** (2008) 014503, [[arXiv:0803.0797](#)].
51. R. Crewther, P. Di Vecchia, G. Veneziano, and E. Witten, *Chiral Estimate of the Electric Dipole Moment of the Neutron in Quantum Chromodynamics*, *Phys.Lett.* **B88** (1979) 123.
52. T. R. Hemmert, M. Procura, and W. Weise, *Quark mass dependence of the nucleon axial vector coupling constant*, *Phys.Rev.* **D68** (2003) 075009, [[hep-lat/0303002](#)].
53. R. Jaffe, *The Axial Anomaly and the Sum Rules for Spin Dependent Electroproduction*, *Phys.Lett.* **B193** (1987) 101.
54. **LHPC Collaborations** Collaboration, P. Hagler *et. al.*, *Nucleon Generalized Parton Distributions from Full Lattice QCD*, *Phys.Rev.* **D77** (2008) 094502, [[arXiv:0705.4295](#)].
55. M. Praszalowicz, H.-C. Kim, and K. Goeke, *SU(3) symmetry breaking and polarized parton densities*, [hep-ph/0110135](#).
56. M. Anselmino, M. Boglione, U. D'Alesio, A. Kotzinian, S. Melis, *et. al.*, *Transversity and Collins Fragmentation Functions: Towards a New Global Analysis*, [arXiv:0807.0173](#).
57. R. Edwards, G. Fleming, P. Hagler, J. W. Negele, K. Orginos, *et. al.*, *Nucleon structure in the chiral regime with domain wall fermions on an improved staggered sea*, *PoS LAT2006* (2006) 121, [[hep-lat/0610007](#)].
58. **for RBC and UKQCD Collaborations** Collaboration, S. Ohta and T. Yamazaki, *Nucleon structure with dynamical (2+1)-flavor domain wall fermions lattice QCD*, [arXiv:0810.0045](#).
59. H.-W. Lin, T. Blum, S. Ohta, S. Sasaki, and T. Yamazaki, *Nucleon structure with two flavors of dynamical domain-wall fermions*, *Phys.Rev.* **D78** (2008) 014505, [[arXiv:0802.0863](#)].
60. **QCDSF Collaboration, UKQCD Collaboration** Collaboration, M. Gockeler *et. al.*, *Quark helicity flip generalized parton distributions from two-flavor lattice QCD*, *Phys.Lett.* **B627** (2005) 113–123, [[hep-lat/0507001](#)].
61. M. Burkardt, A. Miller, and W.-D. Nowak, *Spin-polarized high-energy scattering of charged leptons on nucleons*, *Rept.Prog.Phys.* **73** (2010) 016201, [[arXiv:0812.2208](#)].
62. A. Khan, M. Gockeler, P. Hagler, T. Hemmert, R. Horsley, *et. al.*, *Axial and tensor charge of the nucleon with dynamical fermions*, *Nucl.Phys.Proc.Suppl.* **140** (2005) 408–410, [[hep-lat/0409161](#)].
63. H.-W. Lin and K. Orginos, *First Calculation of Hyperon Axial Couplings from Lattice QCD*, *Phys.Rev.* **D79** (2009) 034507, [[arXiv:0712.1214](#)].
64. J. Foley, K. Jimmy Juge, A. O’Cais, M. Peardon, S. M. Ryan, *et. al.*, *Practical all-to-all propagators for lattice QCD*, *Comput.Phys.Commun.* **172** (2005) 145–162, [[hep-lat/0505023](#)].
65. G. S. Bali, S. Collins, and A. Schafer, *Effective noise reduction techniques for disconnected loops in Lattice QCD*, *Comput.Phys.Commun.* **181** (2010) 1570–1583, [[arXiv:0910.3970](#)].